JACS
JOURNAL OF THE AMERICAN CHEMICAL SOCIETY

ARTICLE

pubs.acs.org/JACS

Enantiomeric Interactions between Liquid Crystals and Organized Monolayers of Tyrosine-Containing Dipeptides

Yiqun Bai and Nicholas L. Abbott*

Department of Chemical and Biological Engineering, University of Wisconsin—Madison, 1415 Engineering Drive, Madison, Wisconsin 53706, United States

Supporting Information

ABSTRACT: We have examined the orientational ordering of nematic liquid crystals (LCs) supported on organized monolayers of dipeptides with the goal of understanding how peptide-based interfaces encode intermolecular interactions that are amplified into supramolecular ordering. By characterizing the orientations of nematic LCs (4-cyano-4′-pentylbiphenyl and TL205 (a mixture of mesogens containing cyclohexane-fluorinated biphenyls and fluorinated terphenyls)) on monolayers of L-cysteine-L-tyrosine, L-cysteine-L-phenylalanine, or L-cysteine-L-phosphotyrosine formed on crystallographically textured films of gold, we conclude that patterns of hydrogen bonds generated by the organized monolayers of dipeptides are transduced via macroscopic orientational ordering of the LCs. This conclusion is supported by the observation that the ordering exhibited by the achiral LCs is specific to the enantiomers used to form the dipeptide-based monolayers. The dominant role of the −OH group of tyrosine in dictating the patterns of hydrogen bonds that orient the LCs was also evidenced by the effects of phosphorylation of the tyrosine on the ordering of the LCs. Overall, these results reveal that crystallographic texturing of gold films can direct the formation of monolayers of dipeptides with long-range order, thus unmasking the influence of hydrogen bonding, chirality, and phosphorylation on the macroscopic orientational ordering of LCs supported on these surfaces. These results suggest new approaches based on supramolecular assembly for reporting the chemical functionality and stereochemistry of synthetic and biological peptide-based molecules displayed at surfaces.

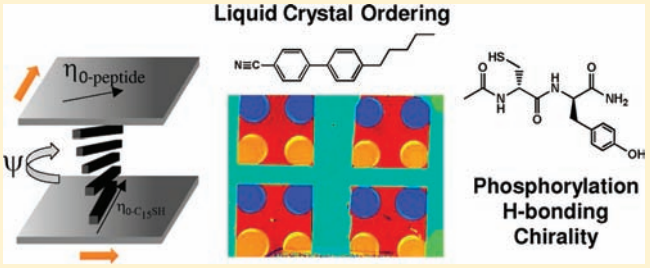

INTRODUCTION

Supramolecular assemblies formed via the collective effects of weak physical interactions (e.g., van der Waals interactions and hydrogen bonds) underlie a range of soft materials that are exquisitely sensitive to chemical stimuli and external fields.[1−5] When supramolecular assemblies exhibit long-range orientational ordering, such as seen within liquid crystalline phases, molecular details such as chirality can be amplified into mesoscopic phenomena.[6−11] At interfaces, in particular, the ordering of liquid crystals (LCs) is widely known to be remarkable for (i) the scale of interfacial energetics that controls the phenomenon (typically $10^{-3}-10^{-6}$ J/m^2) and (ii) the distance over which the ordering of LCs can propagate from interfaces (∼100 μm or ∼10^5 molecular lengths).[12,13] Inspired by the sensitivity of the ordering of LCs to the chemical functionality and organization of molecules at interfaces, a recent series of studies have examined the ordering of LCs on surfaces decorated with oligopeptides,[14−16] proteins,[17−21] DNA,[22,23] viruses,[24] and other biological species. Although observations of surface-induced orientations of LCs at biomolecular interfaces suggest the basis of new ways to couple supramolecular ordering to biomolecules and their transformations (e.g., for reporting such transformations), the complexity of the biomolecules studied in the past has hindered identification of the underlying patterns of intermolecular forces responsible for the observed supramolecular ordering of the LCs.[14−25]

In contrast to past investigations of interfaces comprised of complex biomolecules and their assemblies, studies of simple and structurally well-defined interfaces have succeeded in identifying a range of intermolecular interactions that influence surface-induced orientations of LCs.[12,13,26−30] Of particular relevance to the study reported herein, a series of studies that have employed the self-assembly of organothiol compounds on the surface of gold films have revealed the roles of van der Waals interactions,[31] metal ion−ligand coordination interactions,[32] electrical double layers,[29,30] hydrogen bonding,[26,30] and other intermolecular interactions on the ordering of LCs.[27,28] In this paper, we build from these past studies to examine the ordering of LCs on surfaces decorated with dipeptides. We hypothesized that the simpler structure of the dipeptides, as compared to full proteins and their assemblies, and the ability to make systematic modification to the structure and chirality of the dipeptides would permit us to obtain insight into the intermolecular interactions that underlie the ordering of LCs on peptide-decorated surfaces. As discussed later in this paper, the knowledge gained from these

Received: September 22, 2011
Published: November 17, 2011

dx.doi.org/10.1021/ja2089475 | J. Am. Chem. Soc. 2012, 134, 548–558

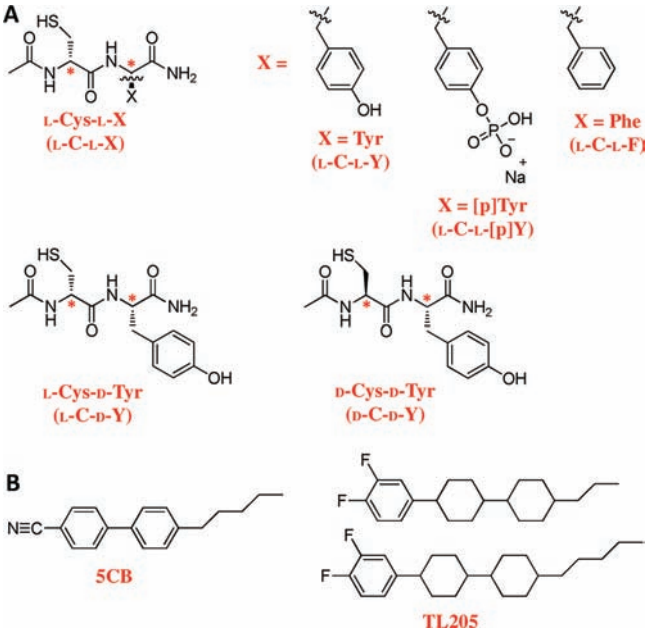

Figure 1. Chemical structures of (A) dipeptides (an asterisk denotes the position of a chiral center) and (B) mesogens used in the studies reported in this paper.

fundamental studies provides guidance to the design of interfaces at which the chemical functionality and stereochemistry of peptide-based synthetic and biological molecules (e.g., proteins) can be reported via the ordering of LCs.

The advances reported in this paper are threefold.

First, we provide insight into the orientational ordering and underlying intermolecular interactions between nematic 4-cyano-4′-pentylbiphenyl (5CB) and surfaces decorated with L-cysteine-L-tyrosine (L-C-L-Y) (Figure 1A). These studies were performed on gold films that were deposited at an oblique angle of incidence. Such gold films have been shown previously to possess in-plane crystallographic texturing that introduces long-range order into monolayers formed on their surfaces.[31,33] A series of experiments reported in this paper that involve comparisons of the orientations of 5CB on several different dipeptide-decorated surfaces support the hypothesis that patterns of hydrogen bonds formed between the nitrile group of 5CB and the −OH group of L-tyrosine play a key role in directing the orientation of the LC on monolayers formed from L-C-L-Y. Further support for the hypothesis is obtained from experiments in which a strong hydrogen bond acceptor (triethylamine) is doped into 5CB and from experiments performed with TL205 (a nematic LC phase formed from a mixture of mesogens comprised of cyclohexane-fluorinated biphenyls and fluorinated terphenyls).

The second advance reported in this paper revolves around the influence of the chirality of the dipeptides on the orientational ordering of the LCs. Studies in which we manipulate the chirality of the amino acids used to synthesize the dipeptides (e.g., L-C-L-Y vs L-C-D-Y vs D-C-D-Y) reveal striking effects on the macroscopic ordering of the LCs. These results indicate that the chirality of the dipeptides influences the patterns of hydrogen bonds presented by the dipeptide-decorated surfaces, an interaction that ultimately directs the ordering of LCs on these surfaces.

The third advance reported in this paper builds from the above two insights by demonstrating that phosphorylation of the tyrosine causes measurable changes in the orientational ordering of LCs on these surfaces. This result shows that chemical modifications leading to alterations in the patterns of hydrogen bonds presented by the dipeptide-decorated surfaces are transduced by the supramolecular assembly of the LC. We note that phosphorylation of tyrosine is an important post-translational modification to proteins in intracellular environments, and the development of new methods to report changes in the phosphorylation of proteins and peptides (or post-translational modifications, more generally) could advance the understanding of intracellular signaling pathways.[34−37]

In the sections reported below, we first report comparisons of the ordering of LCs on various dipeptide-decorated surfaces (including surfaces presenting phosphorylated dipeptides). Subsequently, we describe experiments that provide insights into the intermolecular interactions underlying these observations as well as the effects of the chirality of the dipeptides.

MATERIALS AND METHODS

Materials. Unless noted otherwise, all materials were used as received. Silicon wafers were purchased from Silicon Sense (Nashua, NH). Glass slides (1 in. × 3 in.) were cut from sheets of Corning Eagle 2000 glass from Delta Technologies (Stillwater, MN). Gold (99.999% purity) was obtained from International Advanced Materials (Spring Valley, NY). Titanium (99.99% purity) was obtained from PureTech (Brewster, NY). Decanethiol ($C_{10}SH$), pentadecanethiol ($C_{15}SH$), hexadecanethiol ($C_{16}SH$), triethylamine, and triethanolamine were obtained from Sigma-Aldrich (Milwaukee, WI). Liquid crystals of 5CB and TL205 were obtained from EMD (Hawthorne, NY). TL205 is a mixture of mesogens containing cyclohexane-fluorinated biphenyls and fluorinated terphenyls with aliphatic chains containing 2−5 carbons.[26] Anhydrous ethanol containing 5% isopropyl alcohol and 5% methanol as denaturants was obtained from Sigma-Aldrich and purged with argon gas for 1 h prior to use. Poly(dimethylsiloxane) (PDMS) stamps were prepared using a Sylgard 184 silicone elastomer kit obtained from Dow Corning (Midland, MI). Dipeptides were purchased from New England Peptide (Gardner, MA) and SBS Genetech (Beijing, China) with acetylated N-termini and amidated C-termini. Matrix-assisted laser desorption ionization time-of-flight (MALDI-TOF) analysis was reported by both New England Peptide and SBS Genetech to be within 0.1% of the calculated molecular weight. The purity of the peptides was found to be >95%, as determined by analytical high-performance liquid chromatography (HPLC).

Preparation of Gold Substrates. Briefly, piranha-cleaned glass slides were positioned within the chamber of an electron-beam evaporator (VES-3000-C manufactured by Tek-Vac Industries, Brentwood, NY) such that the angle (θ_i, with respect to the surface normal) at which both titanium (Ti) and gold (Au) were deposited onto the glass slides was specified with an accuracy of ±1°.[25,38] Semitransparent gold films (used for optical measurements of LC orientations) were prepared by sequentially depositing 8 nm of Ti and 20 nm of Au. The films were deposited at an angle of incidence of 35° ± 1°. Reflective gold films prepared using 10 nm Ti and 200 nm Au were used for ellipsometry, X-ray photoelectron spectroscopy (XPS), and polarization modulation infrared reflection−absorption spectroscopy (PM-IRRAS). The latter films were deposited at normal incidence. All gold films were used within 1 h of removal from the evaporator chamber.

Preparation of Dipeptide-Modified Surfaces. Prior to formation of monolayers of dipeptide on the gold films, monolayers formed from hexadecanethiol ($C_{16}SH$) were patterned onto the edge regions of the gold films by using microcontact printing (see the Supporting Information for details). As described below, the monolayers formed from $C_{16}SH$ (i) served to confine aqueous droplets of the dipeptides

dx.doi.org/10.1021/ja2089475 |J. Am. Chem. Soc. 2012, 134, 548–558

placed onto the gold films and (ii) served as reference regions on the surfaces for quantifying the orientations of the LCs.[15,18,19,26,38] The dipeptides were prepared in aqueous 0.1 M triethanolamine buffer (pH 7.2, 500 μM dipeptide), and droplets of the dipeptide solutions were placed by hand pipetting onto the gold films (due to hand pipetting, the droplets were not exactly circular). The dipeptide-modified surfaces were then incubated on the gold films for 23 h. After incubation, the surfaces were rinsed sequentially in deionized water, aqueous HCl (pH 4.2), and then deionized water (pH 5−6). We used the aqueous HCl solution to rinse the gold films because we have observed that acidic solutions (unpublished data) aid in the removal of peptides bound to surfaces through physical interactions. As our observations regarding the ordering of the LC are confined to areas of the surface within the approximately circular regions defined by the droplets, the ordering of the LC between the circular regions does not impact the interpretation of our experiments.

Ellipsometry. The optical thicknesses of the films formed by dipeptides immobilized on 200 nm thick films of gold (see above) were determined by using a Rudolph AutoEL II ellipsometer (wavelength 632 nm, angle of incidence 70°, Rudolph Technologies, Flanders, NJ). The average thickness was determined by measuring three locations on three samples. Error bars represent the standard deviation over the nine measurements. The ellipsometric constants of each batch of gold films were determined by performing an ellipsometric measurement on a piece of a gold film on which a monolayer of $C_{16}SH$ was formed. By using literature values for the thickness of the $C_{16}SH$ monolayer (2.3 nm),[39] the ellipsometric constants of the gold films were calculated. For the calculation of the optical thickness of a dipeptide film, the refractive index was assumed to be $n = 1.46$.[17,40]

X-ray Photoelectron Spectroscopy. XPS was used to determine the atomic composition of the dipeptide-decorated surfaces. The instrument used for the measurements was a Perkin-Elmer PHI 5400 XPS system equipped with an Omni-Focus Lens and a magnesium X-ray source (1486.6 eV). The XPS spectra were obtained over a surface area of approximately 1 mm × 3 mm. Survey scans with a pass energy of 89.45 eV were first performed to identify the elements present on the surface, followed by acquisition of element-specific spectra with a pass energy of 44.75 eV. The major peaks of interest were Au (4f), O (1s), C (1s), N (1s), and P (2p). Data analysis was performed using the RBD Instruments AugerScan (Bend, OR) analysis software. The percentage composition of each element present on the surface was determined, after establishment of the baselines, by integrating the area under each peak and correcting for the element-specific PHI sensitivity factors.[41]

Polarization Modulation Infrared Reflection−Absorption Spectroscopy. Infrared spectra of the dipeptide monolayers formed on gold films (thickness of 200 nm) were obtained using a Nicolet Magna-IR 860 FT-IR spectrometer with a photoelastic modulator (PEM-90, Hinds Instruments, Hillsboro, OR), a synchronous sampling demodulator (SSD-100, GWC Technologies, Madison, WI), and a liquid N_2-cooled mercury cadmium telluride (MCT) detector. All spectra were taken at an incident angle of 83° with the modulator centered at 1500 cm^{-1}. For each sample, 1000 scans were taken at a resolution of 4 cm^{-1}. Quantitative analysis was performed using Mathematica to normalize the baselines, and the results were plotted in Igor Pro.

Fabrication of Optical Cells. Optical cells used for quantification of the orientation of the LCs on dipeptide-modified gold films were fabricated by pairing each dipeptide-modified surface with a reference surface.[15,18,19] The reference surface was a gold film (deposited at an angle of 64° relative to the surface normal) that was functionalized with a 1 mM ethanolic solution of pentadecanethiol ($C_{15}SH$) for 18 h. As described previously, the reference surface was selected to strongly anchor nematic 5CB in an azimuthal direction that was perpendicular to the direction of incidence of the gold during deposition of the gold film (see the Results for an additional description).[15,18,19] The dipeptide-decorated surfaces and reference surfaces were spaced apart using

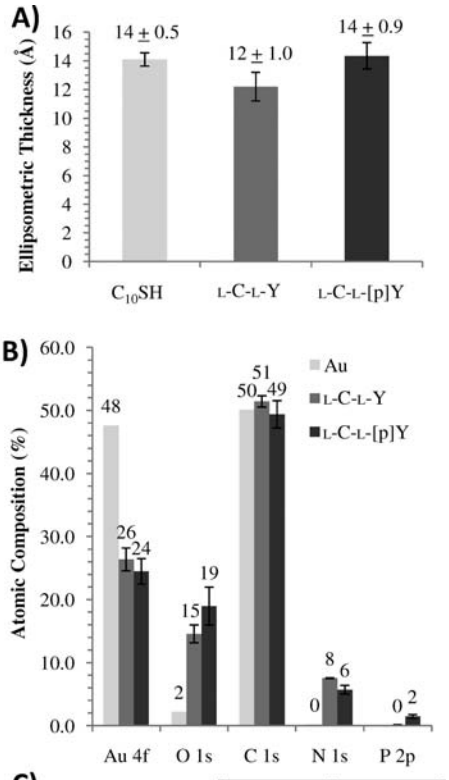

C)

	O:N	P:N
L-C-L-Y (calculated)	1.33	0
L-C-L-Y (actual)	1.9 ± 0.2	0
L-C-L-[p]Y (calculated)	2.33	0.33
L-C-L-[p]Y (actual)	3.3 ± 1.1	0.25 ± 0.1

Figure 2. (A) Ellipsometric thickness of monolayers formed from $C_{10}SH$, L-C-L-Y, or L-C-L-[p]Y. (B) XPS data for dipeptide monolayers adsorbed to Au surfaces. Error bars represent the standard deviations over three independent samples. (C) Calculated and measured O:N and P:N ratios based on XPS data shown in (B).

poly(ethylene terephthalate) (PET) spacers with a thickness of 50 μm. The LCs were heated to the isotropic phase and drawn into the cavity between the two surfaces via capillary action. The samples were cooled to room temperature (25 °C) prior to imaging, as detailed below.

Measurements of the Orientations of LCs. In the majority of the measurements reported in this paper, the azimuthal orientation of the LC at the dipeptide-decorated surface of the optical cells (see above) differed from that at the reference surface (both surfaces caused planar anchoring of the LCs). These boundary conditions induced a twist distortion in the LC, and we define the twist angle of the LC as the change in azimuthal orientation of the director of the LC upon moving from the reference surface to the dipeptide-decorated surface. As detailed previously,[18] we measured the twist angle (ψ) at each pixel of a polarized light micrograph (transmission mode) of the film of LC by rotation of the analyzer and polarizer to minimize the transmission of light through each pixel. A detailed description of the procedure can be found in the Supporting Information. A color map of the twist angles of the LC measured across each sample was constructed by assigning a specific color to each value of the twist angle.[18] In this paper, we report the azimuthal orientation of the LCs on the dipeptide-decorated regions of the surface as the difference between the twist angle of the LCs on the dipeptide- and $C_{16}SH$-decorated regions of the surface (the orientation of LCs on gold films with a monolayer of $C_{16}SH$ corresponds to the

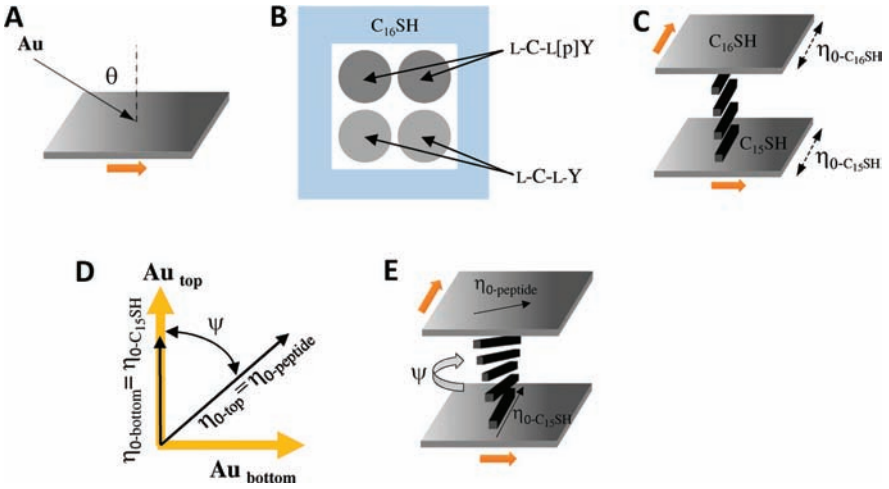

Figure 3. (A) Schematic illustration of physical vapor deposition of a gold film at an oblique angle of incidence. Gold atoms are incident on the substrate at an angle θ relative to the surface normal. The arrow indicated denotes the direction of deposition of the gold. (B) Schematic illustration of a gold film patterned with dipeptides and $C_{16}SH$. (C) Schematic illustration of an optical cell, where the directions of gold deposition on the top and bottom surfaces of the cell are orthogonal. The top surface supports a monolayer of $C_{16}SH$ and the bottom surface a monolayer of $C_{15}SH$. (D) Angle diagram indicating the directions of gold deposition and easy axes of 5CB (η_0) at the top and bottom surfaces of the optical cell. The bottom surface supports a monolayer of $C_{15}SH$, and the top surface supports a monolayer of dipeptide. ψ indicates the twist angle of the LC. (E) Three-dimensional illustration of the diagram in (D).

direction of gold deposition).[15,18,19,27] In the Supporting Information, we describe additional experiments that established that the orientations of the LCs measured in our experiments correspond to the so-called "easy axes" (i.e., lowest interfacial free energy orientation) of the LCs.

RESULTS

Preparation and Characterization of Dipeptide-Decorated Surfaces. Many past studies have investigated the adsorption of amino acids and oligopeptides onto inorganic surfaces.[42−51] Of particular relevance to this paper, several of these studies have reported that cysteine-containing oligopeptides bind strongly to the surfaces of gold films,[42] resulting in the formation of monolayers.[44,50] The first measurements that we report in this paper were performed to confirm that dipeptides containing cysteine and either tyrosine or phosphotyrosine (Figure 1A) formed monolayers with similar surface coverage on the gold films used in our study (see the Materials and Methods for details regarding the deposition of the gold films; a detailed discussion of the structure of the gold films is presented in the Discussion). Specifically, we sought to determine if differences in coverage of the dipeptides on the gold films might underlie some of the results reported below regarding the orientations of LCs on dipeptide-decorated surfaces. Here we note also that the dipeptides used in our experiments were protected via N-terminal acetylation and C-terminal amidation. We used end group protection to eliminate potential changes in the extent of ionization of the terminal carboxylic acid and amine groups of unprotected dipeptides.[52]

Figure 2A reports the ellipsometric thicknesses of dipeptide films formed by incubation of aqueous solutions of either L-C-L-Y or L-C-L-[p]Y on the gold surfaces. As a reference, we also measured the ellipsometric thickness of a monolayer formed from decanethiol ($C_{10}SH$) on the same gold films. The optical thicknesses of the films formed from L-C-L-Y and L-C-L-[p]Y were determined to be 12 ± 1.0 and 14 ± 0.9 Å, respectively, and similar to the ellipsometric thickness of the monolayer formed from $C_{10}SH$ (14 ± 0.5 Å). The similar values of the ellipsometric thicknesses measured for L-C-L-Y and L-C-L-[p]Y are thus consistent with the formation of monolayers of L-C-L-Y and L-C-L-[p]Y of comparable coverage on the surface of the gold films.

Figure 2B shows the XPS spectra of the gold films prior to and after incubation with each dipeptide, revealing an attenuation of the Au signal that indicates the adsorption of the dipeptides (at similar levels of surface coverage) onto the gold surface. We also compared the increase in each of the N 1s, O 1s, and P 2p signals in the XPS spectra to the calculated elemental composition of the dipeptides (Figure 2C). Inspection of Figure 2C reveals that the measured O:N ratio is slightly higher than the values calculated for both L-C-L-Y and L-C-L-[p]Y. We suspect the origin of this difference to be trace amounts of water adsorbed to the dipeptide-decorated surfaces. Previous studies have reported water bound (in vacuum) to alkanethiol monolayers terminated with functional groups (e.g., carboxylic acids) that can hydrogen bond to water.[53,54] The calculated P:N ratio shown in Figure 2C is in good agreement with the experimental value.

We also characterized the gold films incubated with L-C-L-Y and L-C-L-[p]Y by using PM-IRRAS (see Figure S1 of the Supporting Information). In brief, we observed the presence of vibrational bands in the absorption spectra that correspond to the amide I and amide II absorption energies,[47,50,55] in addition to vibrations of the aromatic ring of tyrosine.[56−60] The intensities of the amide I and amide II absorption bands for L-C-L-Y and L-C-L-[p]Y were not significantly different (when compared to sample-to-sample variation). We also quantified the ratio of the intensities of the amide I and amide II absorption bands, and we found no substantial difference between L-C-L-Y and L-C-L-[p]Y. As noted above, a peak corresponding to the vibrations of the aromatic ring of tyrosine was observed at 1518 cm^{-1},[57−60] and the displacement of this peak was measured for L-C-L-[p]Y to 1512 cm^{-1}, consistent with the previously reported effects of phosphorylation.[56] For L-C-L-F, the peak due to the aromatic ring was shifted to 1498 cm^{-1} and was smaller than that of L-C-L-Y.[57,58]

dx.doi.org/10.1021/ja2089475 |J. Am. Chem. Soc. 2012, 134, 548–558

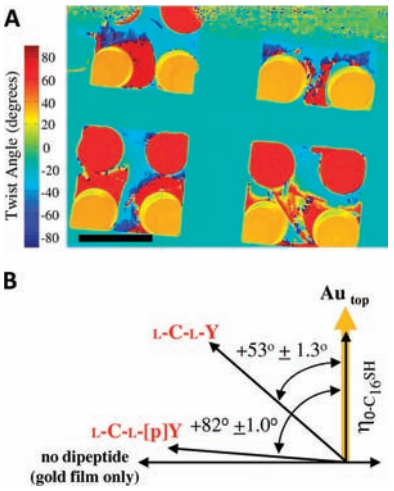

Figure 4. (A) Two-dimensional map of twist angles (see the text) of nematic 5CB on the peptide array shown in Figure 3B. The scale bar is 2 mm. (B) Angle diagram and quantitative analysis of the easy axes of 5CB on L-C-L-Y- and L-C-L-[p]Y-decorated surfaces. The angle diagram indicates the direction of gold deposition on the top surface of the optical cell and the easy axes of 5CB on surfaces decorated with L-C-L-Y and L-C-L-[p]Y or a gold surface without dipeptide. Error bars represent the standard deviations of 220 droplets for L-C-L-Y and 59 droplets for L-C-L-[p]Y.

Overall, the above-described measurements, when combined, lead us to conclude that both L-C-L-Y and L-C-L-[p]Y formed monolayers on the surfaces of the gold films used in our experiments and that the extent of surface coverage of the two dipeptides is similar. Specifically, these results suggest that differences in the orientations of LCs on L-C-L-Y- and L-C-L-[p]Y-decorated surfaces, as described below, are not due to differences in the extent of coverage of the dipeptides on the gold films.

Measurement of the Orientations of Nematic 5CB on Dipeptide-Decorated Surfaces. Next we measured the orientations assumed by nematic 5CB (Figure 1B) in contact with the gold films decorated with monolayers of either L-C-L-Y or L-C-L-[p]Y. The fabrication of the optical cells used to perform these measurements is detailed in the Materials and Methods. In brief, the top surface of the optical cell was a gold film (deposited at an oblique angle of incidence, Figure 3A) onto which both L-C-L-Y and L-C-L-[p]Y were patterned by spotting of aqueous solutions of the dipeptides (Figure 3B). A monolayer formed from hexadecanethiol ($C_{16}SH$) was patterned around the rim of each dipeptide-decorated gold film (also see Figure 3B). The bottom surface that confined the film of LC was a gold film that supported a monolayer formed from $C_{15}SH$. Past studies[27,61] have shown that nematic 5CB, when placed into contact with an obliquely deposited gold film that supports a monolayer formed from $C_{16}SH$, assumes an orientation (in the plane of the surface) that is parallel to the direction of incidence of the gold during deposition of the gold film (top surface shown in Figure 3C); in contrast, the orientation of the easy axis of 5CB on a monolayer of $C_{15}SH$ is perpendicular to the direction of gold deposition (bottom surface shown in Figure 3C). The molecular origins of this "odd−even" effect are detailed in the Discussion. Finally, we note that past studies have also established that the anchoring energy of nematic 5CB on a monolayer of $C_{15}SH$ is high (>10 μJ/m^2).[18,19] Thus, in the experiments reported below, the orientation of the LC on the $C_{15}SH$ monolayer of the bottom surface is invariant (an assumption that is supported by our results).

Table 1. Azimuthal Orientation of the Easy Axes (η_0) of 5CB on Dipeptide-Decorated Surfaces, Determined Relative to the Easy Axis of the LC Measured from a Monolayer Formed from $C_{16}SH$ (i.e., the Direction of Gold Deposition)[a]

LC	Dipeptide	η_0, deg
5CB	L-C-L-Y	53 ± 1.3
	L-C-L-[p]Y	82 ± 1.0
	L-C-L-F	80 ± 0.9
	L-C-D-Y	−22 ± 0.8
	D-C-D-Y	−52 ± 1.6
5CB + 2.5 mM triethylamine	L-C-L-Y	41 ± 1.1
	L-C-L-F	78 ± 1.0

[a] Positive angles indicate a counterclockwise rotation relative to the direction of gold deposition, and negative angles indicate a clockwise rotation.

When fabricating each optical cell, we paired the gold films described above such that the vectors describing the directions of deposition of gold on each film were orthogonal, as shown in Figure 3C. In this configuration, the nematic 5CB orients in the same azimuthal direction at the confining surfaces supporting monolayers formed from $C_{15}SH$ (bottom surface) and $C_{16}SH$ (top surface), resulting in a uniform orientation of the LC across the entire film (as shown by results presented below and depicted in Figure 3C).[18] In contrast, we measured the LC in contact with the dipeptide-decorated regions of the top surface to exhibit a substantial twist distortion (Figure 3D,E). Figure 4A shows a spatial map of the twist angles of nematic 5CB measured over the surface of an obliquely deposited gold film decorated with either L-C-L-Y or L-C-L-[p]Y (the patterning of the surface is shown in Figure 3B). The twist angle of the LC was determined for each pixel of the image of the LC film. Each pixel is 14 μm × 14 μm and is assigned a color according to the color bar shown to the left of Figure 4A. We note that a positive twist angle corresponds to a gold film on which the azimuthal orientation of the LC director was rotated counterclockwise relative to the direction of gold deposition. A key result extracted from Figure 4A is that the regions of the surface incubated against each dipeptide give rise to homogeneous twist angles. A second key result extracted from Figure 4A is that an image of the twist angles of the LC on these surfaces provides a spatial map of the patterned dipeptides.

By using the map of twist angles reported in Figure 4A, we calculated (see the Materials and Methods) the average azimuthal orientation of the easy axis of 5CB on the surfaces presenting L-C-L-Y to be 53° ± 1.3° and L-C-L-[p]Y to be 82° ± 1.0° (Figure 4B; as noted in the Materials and Methods, the angle is measured relative to the direction of deposition of the gold film, which also coincides with the orientation assumed by the LC on a gold film with a monolayer of $C_{16}SH$; see Table 1 for a tabulated summary of orientations of the LC on the various dipeptide-decorated surfaces reported in this paper). We emphasize that the orientations of the LCs on the dipeptide-decorated surfaces were highly reproducible. In particular, the orientations reported above were determined from two separate batches of gold films and the analysis of 220 L-C-L-Y-decorated surfaces and 59 L-C-L-[p]Y-decorated surfaces. The results above lead to three key conclusions. First, the results above indicate that the azimuthal orientation of the LC on the surface presenting

L-C-L-Y is rotated by 37° ± 1.3° (37° = 90° − 53°) relative to that measured on obliquely deposited gold films without a dipeptide monolayer (see Figure 4B). This result reveals that intermolecular interactions between the dipeptide and 5CB have a measurable influence on the orientation of the LC.[62] Second, we note that the orientation assumed by 5CB on the L-C-L-Y-decorated surface is not parallel or perpendicular to the direction of deposition of gold. This result is in contrast with those of all past studies of ω-terminated alkanethiols on gold films in which the easy axes of smectic and nematic LCs have been measured to be either parallel or perpendicular to the direction of deposition of the gold film.[18,19,27,31,38,62,63] This point, which is related to the chirality of the adsorbates, is addressed in detail in the Discussion. Third, we note that there is a substantial difference between the orientations assumed by nematic 5CB on the gold films decorated with either L-C-L-Y or L-C-L-[p]Y. That is, phosphorylation of the tyrosine of the dipeptide leads to a large (29° ± 1.6°; 29° = 82° − 53°) and easily quantified change in the orientation of the LC on the dipeptide-decorated surfaces.

We note that we performed several additional experiments to confirm that the orientations of the LC reported above do correspond to the easy axes of the LC on the dipeptide-decorated surfaces. Specifically, for LC films with thicknesses of 50 μm, we determined that the torque generated by the twist distortion of the LC was sufficiently small that the orientation of the LC measured at the dipeptide-decorated surfaces was not perturbed by the torque (i.e., the measured orientation is the equilibrium orientation of the LC in the absence of a torque).[64] In the interest of brevity, we have placed detailed descriptions of these confirmatory experiments in the Supporting Information (Figures S2 and S3). We note, in addition, that we considered the possibility that the twist angles of the LC reported above might be influenced by desorption of the chiral dipeptides from the surfaces into the LC (thus acting as a chiral dopant in the LC that induces a twist distortion).[65−68] We excluded this possibility by performing measurements with LC films that varied in thickness. The results of these experiments are also presented in the Supporting Information (Figure S4).

Intermolecular Interactions between Nematic 5CB and Dipeptide-Decorated Surfaces. The orientations assumed by nematic 5CB on the surfaces decorated with L-C-L-Y and L-C-L-[p]Y, as described above, reveal that 5CB possesses distinct intermolecular interactions with the L-tyrosine and L-phosphotyrosine of the L-C-L-Y- and L-C-L-[p]Y-decorated surfaces. Here we report a series of experiments performed to provide insight into these intermolecular interactions.

We first chose to test the hypothesis that patterns of hydrogen bonds encoded by the immobilized tyrosine play a role in dictating the ordering of 5CB on these surfaces. We note that previous studies reported by Luk et al. concluded that hydrogen bonding between LCs and COOH-terminated monolayers can influence the orientations of LCs.[26] We also note that nitrile groups bonded to aromatic rings (as present in 5CB) are particularly electron-rich and capable of serving as hydrogen bond acceptors for the OH group of Tyr,[69,70] as evidenced by IR spectroscopy.[71−74] Informed by these previous studies, we hypothesized that patterns of hydrogen bonds between the OH group of the tyrosine and the nitrile group of 5CB may influence the ordering of 5CB on L-C-L-Y-decorated surfaces. To test this hypothesis, we performed an experiment using a dipeptide in which we replaced the tyrosine residue by a phenylalanine residue (F). This dipeptide (L-C-L-F) is identical to L-C-L-Y with the exception that it does not contain an −OH group that can participate in hydrogen bonding with 5CB (Figure 1A). For surfaces decorated with L-C-L-F, van der Waals and $\pi-\pi$ stacking interactions can occur between the aromatic groups of 5CB and Phe.[69]

We measured the orientation of the easy axis of 5CB on obliquely deposited gold films decorated with L-C-L-F to be 80° ± 1.0° (see Table 1 and Figure S5 (Supporting Information) for a map of the twist angles). This orientation of 5CB differs by 27° ± 1.6° from that measured on L-C-L-Y (see also Table 1) and thus supports the proposition that the orientation of nematic 5CB on the surfaces decorated with L-C-L-Y is influenced by hydrogen bonding between the OH group of Tyr and 5CB: in the absence of hydrogen bonding, the orientation of the LC on surfaces decorated with L-C-L-F departs from that measured with L-C-L-Y.

To provide an additional test of the role of hydrogen bonding, we measured the easy axis of 5CB on surfaces decorated with L-C-L-Y and L-C-L-F when the 5CB was doped with 2.5 mM triethylamine, a base with a higher heat of hydrogen bond formation (8.9 ± 0.09 kcal/mol) as compared to a nitrile group (4.2 ± 0.2 kcal/mol).[75] We hypothesized that the presence of a stronger hydrogen bond acceptor would disrupt the easy axis of 5CB on surfaces that form hydrogen bonds with 5CB, but would not change the easy axis of 5CB on surfaces that do not hydrogen bond with 5CB. Indeed, we found the easy axis of 5CB doped with 2.5 mM triethylamine to be 41° ± 1.1° on L-C-L-Y and 78° ± 1.0° on L-C-L-F (see Table 1). Thus, while the easy axis of 5CB with and without triethylamine differed by 12° ± 1.7° on the L-C-L-Y-decorated surfaces, the presence of triethylamine caused no measurable difference in the orientation of 5CB on L-C-L-F-decorated surfaces. Overall, the observations presented above, when combined, provide support for our proposition that patterns of hydrogen bonds formed between L-C-L-Y and 5CB play a key role in determining the ordering of 5CB on the L-C-L-Y-decorated surfaces. We note that while we have established that hydrogen bonding between the LCs and tyrosine influences the orientation of LCs on surfaces decorated with Tyr-containing dipeptides, we do not exclude the possibility that other intermolecular interactions (i.e., $\pi-\pi$ stacking between the aromatic groups of 5CB and Tyr, hydrogen bonding between C═O and NH groups of the dipeptide backbone, and van der Waals interactions) are present in these systems.[76−78] In summary, our experimental results, when combined with prior FTIR studies of hydrogen bonding between benzonitrile and phenol,[71,73,74] support our conclusion that hydrogen bonding between the −OH group of Tyr and 5CB plays a central role in ordering the 5CB.[71,73,74]

Because the spatial patterns of tyrosine that encode the above-proposed hydrogen bonds between the LC and dipeptide-decorated surfaces would be expected to depend on the chirality of the amino acid residues used to synthesize the dipeptides, we next investigated the effects of changes in the chirality of the dipeptides on the orientations of the LC. The dipeptides used in the current study contain two chiral centers (Figure 1A): L-C-L-Y and D-C-D-Y shown in Figure 1 are enantiomers, while L-C-L-Y and L-C-D-Y are diastereomers. Prior to performing measurements of the orientations of the LCs on the surfaces with the various stereoisomers, we also confirmed the formation of monolayers of the dipeptides via the use of PM-IRRAS (Figure S1, Supporting Information). The orientations of 5CB on surfaces decorated with these dipeptides are summarized in Table 1 and Figure 5. Whereas the interactions of 5CB with surfaces

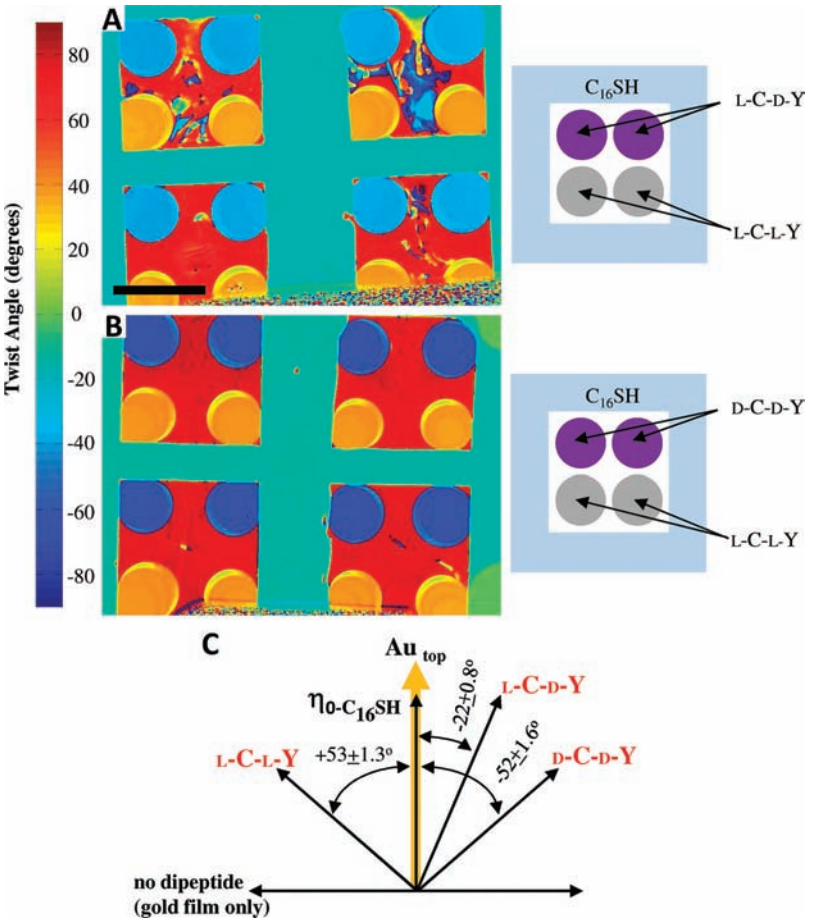

Figure 5. (A) Map of twist angles of nematic 5CB on gold films decorated with monolayers of L-C-L-Y or L-C-D-Y. (B) Map of twist angles of nematic 5CB on gold films decorated with monolayers of L-C-L-Y or D-C-D-Y. The scale bar is 2 mm. (C) Angle diagram and quantitative analysis of the easy axes of 5CB on L-C-L-Y-, L-C-D-Y-, and D-C-D-Y-decorated surfaces. The angle diagram indicates the direction of gold deposition on the top surface of the optical cell and the easy axes of 5CB on surfaces decorated with dipeptides or a gold surface without dipeptide.

decorated with L-C-L-Y caused the azimuthal orientation of the LC to be rotated *counterclockwise* by 53° ± 1.3° relative to the direction of gold deposition, we measured the easy axes of 5CB on surfaces decorated with D-C-D-Y to be rotated *clockwise* by 52° ± 1.6° relative to the direction of gold deposition. Thus, within the precision of the measurement, the magnitude of the rotation of the easy axis of 5CB was indistinguishable. The direction of rotation (handedness), however, was opposite. We also measured the orientations of 5CB on another stereoisomer of L-C-L-Y, namely, L-cysteine-D-tyrosine (L-C-D-Y) (Figure 1A). On these surfaces, we measured the azimuthal orientation of the easy axis of nematic 5CB to be −22° ± 0.8°, a value that is intermediate between those of the two enantiomers L-C-L-Y and D-C-D-Y. We have also investigated the influence of enantiomeric excess in monolayers containing mixtures of L and D stereoisomers. While the details of these studies are beyond the scope of this paper and will be addressed in a subsequent publication, we mention here that a mixture containing 50% L-C-L-Y and 50% D-C-D-Y results in an orientation of the LC that is 0° (i.e., the twisting effect of the chiral dipeptides on the LC is exactly canceled out). Overall, our results support our hypothesis that the chirality of the dipeptides influences the patterning of chemical functional groups at the dipeptide-decorated surfaces and that these differences in patterns lead to intermolecular interactions (specifically, hydrogen bonds) that are reported in the macroscopic orientations exhibited by the LC.

DISCUSSION

The results described above (and see below for additional discussion and evidence) support the hypothesis that the macroscopic orientational ordering of 5CB on surfaces decorated with the dipeptides is encoded by surface patterns of hydrogen bonds formed between the surfaces and LC. We note that these observations arise from experiments performed using dipeptide monolayers formed on gold films deposited at an oblique angle of incidence. As discussed below, we interpret our results to indicate that the crystallographic texturing of the gold films, which is induced by the oblique deposition,[33,62] directs the introduction of long-range order into the monolayers of dipeptides used in our experiments. Previous studies of monolayers formed from organosulfur-containing molecules on gold have also reported lateral interactions (including hydrogen bonding and van der Waals interactions) between the molecules to aid in the formation and organization of the monolayer.[79,80] In our experiments, it is likely that hydrogen bonding between adjacent dipeptides within the monolayer influences the ordering of the monolayer.[76−78] The long-range order within the dipeptide monolayer leads to the patterning of the surface with hydrogen

dx.doi.org/10.1021/ja2089475 |J. Am. Chem. Soc. 2012, 134, 548–558

bonds such that phosphorylation of the tyrosine and the stereochemistry of the amino acids have clear effects on the orientational ordering of the LC.

A number of past studies have investigated surface-induced ordering of LCs on inorganic materials deposited at oblique angles of incidence on planar substrates.[27,28,31,62,81−83] These studies have established that oblique deposition of gold leads to the introduction of nanotopographical features into the surfaces (e.g., associated with the shapes of the gold grains) as well as in-plane and out-of-plane crystallographic texturing of the polycrystalline films.[33,62] For example, by using atomic force microscopy (AFM), Skaife et al. revealed that obliquely deposited gold films possess a subtle level of anisotropy in their nanoscale surface topography, a surface roughness that is greater when measured in a direction parallel to the direction of gold deposition as compared to the perpendicular (in-plane) orientation.[62] In addition to the anisotropic topography, however, obliquely deposited gold films have also been shown to exhibit crystallographic texturing.[33] For example, the Au(111) faces of polycrystalline gold films have been measured to tilt (by up to 5°) toward the direction of deposition of the gold, and optical second-harmonic generation (SHG) measurements indicate in-plane (azimuthal) crystallographic texturing of the gold grains.[31,33]

Past studies of the orientations of LCs provide evidence that both the nanoscopic topography and crystallographic texturing influence the orientations of LCs supported on obliquely deposited gold films.[31,33,62] For example, in the absence of formation of an organic monolayer on an obliquely deposited gold film, it is observed that the azimuthal orientation assumed by 5CB is perpendicular (and in the plane of the surface) to the direction of deposition of the gold film (see Figure 3).[62] This orientation of the LC is consistent with that predicted on the basis of the nanotopographical roughness of the gold film, specifically minimization of the elastic energy associated with distortion of the LC over the roughness of the surface.[62] In short, the LC assumes an azimuthal orientation that is parallel to the direction on the surface that corresponds to minimum roughness. In addition, however, past studies provide evidence that the in-plane crystallographic texturing of the gold films can influence the structure of self-assembled monolayers (SAMs) formed from alkanethiols on the gold films, which in turn impacts the orientational ordering of LCs via intermolecular interactions between the LC and the ordered monolayer.[27,31] In particular, infrared-visible sum-frequency spectroscopic (SFS) measurements show that monolayers of alkanethiols possess macroscopic, in-plane order when formed on obliquely deposited gold films.[31] This long-range order is evidenced by macroscopic azimuthal ordering of the methyl groups of monolayers of alkanethiols formed on the gold films. Related to this conclusion, it has been observed that monolayers formed from alkanethiols that possess an even number of carbon atoms template an orientation of nematic 5CB that is parallel to the direction of deposition of the gold film. Such an orientation of the LC cannot be understood on the basis of the influence of the nanoscopic topography of the surface on the LC mentioned above, but is consistent with the presence of long-range order in the organic monolayers formed on obliquely deposited films of gold and intermolecular interactions (e.g., van der Waals) between the monolayer and LC that influence the ordering of the LC.[27,62] The results presented in this paper, as discussed below, are also consistent with the presence of long-range order within monolayers formed by dipeptides on obliquely deposited gold films.

A key finding reported in this paper is that LCs exhibit uniform azimuthal orientations on dipeptide-decorated gold films that do not lie perpendicular to the direction of deposition of the gold (i.e., the orientation of the LC consistent with the effects of the nanotopography). Similar to the above-mentioned reports of the orientations of LCs on monolayers formed from alkanethiols,[27,28,31,62,81−83] this result suggests that the monolayers of dipeptides formed on the obliquely deposited films possess a macroscopic ordering induced by the crystallographic texturing of the gold films. However, a key additional observation reported in this paper is that the orientation of nematic 5CB on obliquely deposited gold films decorated with L-C-L-Y is rotated counterclockwise by an angle of 53° ± 1.3° from the direction of gold deposition. As noted above, in past studies of ω-functionalized alkanethiols that possessed long-range order on obliquely deposited gold films,[27,31] the effects of crystallographic texturing on the ordering of the monolayers were observed to lead to an azimuthal orientation that was always parallel to the direction of deposition of the gold. Our observation that the L-C-L-Y-decorated surfaces cause nematic LCs to depart from this azimuthal orientation highlights a fundamental difference in the nature of the ordering of LCs on the two sets of surfaces (alkanethiols versus dipeptides). A key difference between these two classes of monolayers is that the ω-functionalized alkanethiols used in past studies were achiral, whereas the dipeptides used in this study possess two chiral centers. In the absence of chirality, the monolayers formed on the gold films possess a mirror plane that contains the vector describing the direction of deposition of the gold films. This symmetry is consistent with the results of the above-mentioned SFG measurements[31] as well as the orientations assumed by the LC on monolayers of achiral molecules.[27,38] In contrast, on surfaces presenting monolayers of chiral molecules that possess long-range order, the chirality of the molecules breaks the in-plane mirror symmetry, and thus, LCs are observed to exhibit orientations that depart from those observed with achiral molecules. The role of the chirality of the peptides is clearly demonstrated in our experiments by the observation that the orientation of nematic 5CB on obliquely deposited gold films decorated with D-C-D-Y is rotated *clockwise* whereas the orientation of the LC is rotated *counterclockwise* by L-C-L-Y.

We note that several previous studies have reported on the influence of chirality on the ordering of LCs at surfaces.[6−8,11] For example, a rich literature addresses chirality in bent-core LC systems,[10,11] and more recently, the alignment of achiral nematic LCs on chiral surfaces has also been reported.[6−8] One such study is based on the mechanical generation of mesoscale surface chirality,[7,8] where the tip of an atomic force microscope was used to scribe a chiral pattern into a polymer-coated surface. The chiral alignment of nematic LCs on these surfaces was reported. Alternatively, the uniform shearing (and resulting macroscopic alignment) of double-stranded DNA films on surfaces has also been observed to cause ordering of LCs in a manner that reflects the chirality of the DNA.[8] Although these recent studies demonstrate that chiral molecules deposited on surfaces can induce preferred orientations of achiral nematic LCs, we note several significant differences between the work presented in this paper and these past studies. In particular, the dipeptide monolayers described in this paper are formed by self-assembly rather than the use of external shear (mechanical) forces. In our system, the azimuthal degeneracy of the surface is broken by the crystallographic texturing of the gold film. Our observations indicate that the anisotropic structure of the gold film provides a field that

directs the assembly of the dipeptides on the surface into monolayers that possess macroscopic organization. In addition, our study is based on dipeptides, and we demonstrate that chemical modifications to the dipeptide structure (e.g., phosphorylation) have pronounced effects on their interactions with LCs.

We conclude this discussion by noting again that a key observation reported in this paper is that the orientations of the LC are strongly influenced by patterns of hydrogen bonds formed between the LC and dipeptides at the surfaces. Evidence in support of this proposition is provided by experiments in which we replaced the tyrosine residue by a phenylalanine residue (L-C-L-Y to L-C-L-F). In addition, the observation that the orientation of 5CB on D-C-D-Y differed from that on L-C-L-Y provides further support for the conclusion that the LC is transducing the patterns of chemical functional groups presented at the dipeptide-decorated surfaces. We note also that we performed additional tests of the role of hydrogen bonding on the orientations of LCs by using the liquid crystal TL205 (Figure 1B). In contrast to 5CB, the mesogens comprising TL205 do not possess nitrile groups but instead possesses fluorinated aromatic rings to induce polarity in the mesogens.[84] Although the dipoles associated with the fluorines (dipole moment μ = 1.5D)[85] are generally weaker than those of nitriles (μ = 3.6D),[85] previous studies have demonstrated that fluorinated aromatic groups (as present in TL205) can serve as hydrogen bond acceptors.[86] We measured the easy axis of TL205 on L-C-L-F-decorated surfaces and found it to be 84° ± 0.6°, similar to the easy axis of 5CB on L-C-L-F (Table 1; Figure S5B, Supporting Information). In contrast, the easy axis of TL205 on L-C-L-Y was 26° ± 1.6°, an orientation that differs by 58° ± 1.7° from the easy axis of TL205 on L-C-L-F. The observation that TL205 assumes distinct azimuthal orientations on the gold films decorated with L-C-L-Y and L-C-L-F is consistent with our hypothesis that the fluorine groups of TL205 form hydrogen bonds with the −OH groups of tyrosine. These experiments thus provide a second example of the influence of hydrogen bonding involving the −OH group of Tyr on the orientational ordering of LCs.

We also conclude that a consequence of the dominant role of hydrogen bonding on ordering of nematic 5CB on the dipeptide-decorated surfaces is that chemical modifications to the dipeptides that change the capacity of the dipeptides to participate in hydrogen bonds lead to macroscopic ordering transitions in the LC. This is evidenced by our observation that phosphorylation of the tyrosine led to a distinct change in the orientation of the LC (see Table 1). Here we note that the pK_a of phosphotyrosine (corresponding to a change in charge from −2 to −1) is 5.8 in bulk aqueous solution,[87,88] although past studies have demonstrated that the ionization behaviors of acids at surfaces are substantially different as compared to those in bulk solutions.[29] For example, for carboxylic acids, the extent of ionization of the acids is incomplete 5 pH units above the bulk solution pK_a (4.5).[29] Thus, at the pH of the aqueous solution used as the final rinse of the dipeptide-decorated surfaces (pH 5−6), it is likely that the phosphate of phosphotyrosine has one P−OH group.[87] Although this state of the phosphate group may permit hydrogen bonding with the 5CB, our results indicate that hydrogen bonding between 5CB and the phosphate, if it does take place, has an influence that is distinct from that of hydrogen bonding with the tyrosine. A possible explanation for this result is that, in contrast to tyrosine, the phosphate group possesses rotational freedom, thus preventing the formation of hydrogen bonds that have a well-defined orientation with respect to the surface. Although additional studies are required to fully understand the interactions of phosphotyrosine and 5CB, the ability to directly detect the phosphorylation status and chirality of peptides on surfaces, through the macroscopic orientations exhibited by LCs, suggests the basis of new approaches based on supramolecular assembly for reporting the chemical functionality and stereochemistry of biomolecules displayed on surfaces.

CONCLUSIONS

We have described a series of studies that characterize and provide insight into the intermolecular interactions that influence the ordering of thermotropic LCs on dipeptide-decorated surfaces. In particular, our results suggest that hydrogen bonding between 5CB and TL205 and tyrosine plays a central role in determining the orientations assumed by LCs on tyrosine-decorated surfaces. Phosphorylation of the tyrosine, as well as changes in the chirality of amino acids used to form the dipeptides, have pronounced effects on the orientational ordering of LCs because these modifications alter the patterns of hydrogen bonds presented by the dipeptide. We infer from our observations of the ordering of LCs on the dipeptide-decorated surfaces that long-range order is present within the dipeptide monolayers used in our studies and that this long-range ordering of the dipeptides is directed by the crystallographic texture of the underlying obliquely deposited gold films. Overall, the results presented in this paper advance our understanding of the intermolecular interactions that underlie the ordering of LCs on peptide-decorated surfaces. Our results also suggest that investigations of the orientations of LCs on monolayers formed from biomolecules can offer the basis of novel methodologies that can provide fundamental insights into the chemical functionality and stereochemistry of the synthetic and biological peptide-based systems.

ASSOCIATED CONTENT

Supporting Information. Additional figures discussed in the text. This material is available free of charge via the Internet at: http://pubs.acs.org/.

AUTHOR INFORMATION

Corresponding Author
abbott@engr.wisc.edu

ACKNOWLEDGMENT

This work was supported by the National Science Foundation (NSF) under Awards DMR-1121288 (MRSEC), by the National Institutes of Health (Grants CA108467 and AI092004) and by the Army Research office (W911NF-11-1-0251). Y.B. acknowledges the receipt of a graduate fellowship from the NSF. We thank Aaron Lowe, Sandro Mecozzi, and Samuel Gellman for helpful discussions and Aaron Lowe for careful reading of the manuscript.

REFERENCES

(1) Chen, R. J.; Choi, H. C.; Bangsaruntip, S.; Yenilmez, E.; Tang, X.; Wang, Q.; Chang, Y.-L.; Dai, H. *J. Am. Chem. Soc.* **2004**, *126*, 1563–1568.

(2) Hoogboom, J.; Garcia, P. M. L.; Otten, M. B. J.; Elemans, J.; Sly, J.; Lazarenko, S. V.; Rasing, T.; Rowan, A. E.; Nolte, R. J. M. *J. Am. Chem. Soc.* **2005**, *127*, 11047–11052.

(3) Herrwerth, S. E., W.; Reinhardt, S.; Grunze, M. *J. Am. Chem. Soc.* **2003**, *125*, 9359–9366.
(4) Charych, D. H.; Nagy, J. O.; Spevak, W.; Bednarski, M. D. *Science* **1993**, *261*, 585−588.
(5) Bai, Y.; Abbott, N. L. *Langmuir* **2011**, *27*, 5719–5738.
(6) Choi, Y.; Atherton, T.; Ferjani, S.; Petschek, R. G.; Rosenblatt, C. *Phys. Rev. E* **2009**, *80*, 060701.
(7) Ferjani, S.; Choi, Y.; Pendery, J.; Petschek, R. G.; Rosenblatt, C. *Phys. Rev. Lett.* **2010**, *104*, 257801.
(8) Nakata, M.; Zanchetta, G.; Buscaglia, M.; Bellini, T.; Clark, N. A. *Langmuir* **2008**, *24*, 10390–10394.
(9) Takezoe, H. In Topics in Current Chemistry Springer: Berlin/Heidelberg, 2011 pp 1−28.
(10) Hough, L. E.; Spannuth, M.; Nakata, M.; Coleman, D. A.; Jones, C. D.; Dantlgraber, G.; Tschierske, C.; Watanabe, J.; Korblova, E.; Walba, D. M.; Maclennan, J. E.; Glaser, M. A.; Clark, N. A. *Science* **2009**, *325*, 452–456.
(11) Shiromo, K.; Sahade, D. A.; Oda, T.; Nihira, T.; Takanishi, Y.; Ishikawa, K.; Takezoe, H. *Angew. Chem., Int. Ed.* **2005**, *44*, 1948–1951.
(12) Cognard, J. *Mol. Cryst. Liq. Cryst.* 1982, *78* (Suppl. 1), 1–77.
(13) Jerome, B. *Rep. Prog. Phys.* **1991**, *54*, 391–451.
(14) Clare, B. H.; Abbott, N. L. *Langmuir* **2005**, *21*, 6451–6461.
(15) Govindaraju, T.; Bertics, P. J.; Raines, R. T.; Abbott, N. L. *J. Am. Chem. Soc.* **2007**, *129*, 11223–11231.
(16) Bi, X. Y.; Lai, S. L.; Yang, K. L. *Anal. Chem.* **2009**, *81*, 5503–5509.
(17) Luk, Y. Y.; Tingey, M. L.; Dickson, K. A.; Raines, R. T.; Abbott, N. L. *J. Am. Chem. Soc.* **2004**, *126*, 9024–9032.
(18) Lowe, A. M.; Bertics, P. J.; Abbott, N. L. *Anal. Chem.* **2008**, *80*, 2637–2645.
(19) Lowe, A. M.; Ozer, B. H.; Bai, Y.; Bertics, P. J.; Abbott, N. L. *ACS Appl. Mater. Interfaces* **2010**, *2*, 722–731.
(20) Xue, C. Y.; Hartono, D.; Yang, K. L. *Langmuir* **2008**, *24*, 11282–11286.
(21) Xue, C. Y.; Khan, S. A.; Yang, K. L. *Adv. Mater.* **2009**, *21*, 198–202.
(22) Chen, C. H.; Yang, K. L. *Langmuir* **2010**, *26*, 1427–1430.
(23) Price, A. D.; Schwartz, D. K. *J. Am. Chem. Soc.* **2008**, *130*, 8188–8194.
(24) Jang, C. H.; Cheng, L. L.; Olsen, C. W.; Abbott, N. L. *Nano Lett.* **2006**, *6*, 1053–1058.
(25) Clare, B. H.; Guzman, O.; de Pablo, J. J.; Abbott, N. L. *Langmuir* **2006**, *22*, 7776–7782.
(26) Luk, Y.-Y.; Yang, K.-L.; Cadwell, K.; Abbott, N. L. *Surf. Sci.* **2004**, *570*, 43–56.
(27) Gupta, V. K.; Abbott, N. L. *Phys. Rev. E* **1996**, *54*, 4540–4543.
(28) Gupta, V. K.; Abbott, N. L. *Langmuir* **1996**, *12*, 2587–2593.
(29) Shah, R. R.; Abbott, N. L. *J. Phys. Chem. B* **2001**, *105*, 4936–4950.
(30) Shah, R. R.; Abbott, N. L. *J. Am. Chem. Soc.* **1999**, *121*, 11300–11310.
(31) Follonier, S.; Miller, W. J. W.; Abbott, N. L.; Knoesen, A. *Langmuir* **2003**, *19*, 10501–10509.
(32) Cadwell, K. D.; Alf, M. E.; Abbott, N. L. *J. Phys. Chem. B* **2006**, *110*, 26081–26088.
(33) Everitt, D. L.; Miller, W. J. W.; Abbott, N. L.; Zhu, X. D. *Phys. Rev. B* **2000**, *62*, R4833–R4836.
(34) Ahn, N. G.; Resing, K. A. *Nat. Biotechnol.* **2001**, *19*, 317–318.
(35) Houseman, B. T.; Huh, J. H.; Kron, S. J.; Mrksich, M. *Nat. Biotechnol.* **2002**, *20*, 270–274.
(36) Trewavas, A. *Annu. Rev. Plant Physiol.* **1976**, *27*, 349–374.
(37) Kia-Ki, H.; Martinage, A. *Int. J. Biochem.* **1992**, *24*, 19–28.
(38) Clare, B. H.; Guzman, O.; de Pablo, J. J.; Abbott, N. L. *Langmuir* **2006**, *22*, 4654–4659.
(39) Rosu, D. M.; Jones, J. C.; Hsu, J. W. P.; Kavanagh, K. L.; Tsankov, D.; Schade, U.; Esser, N.; Hinrichs, K. *Langmuir* **2008**, *25*, 919–923.
(40) Troughton, E. B.; Bain, C. D.; Whitesides, G. M.; Nuzzo, R. G.; Allara, D. L.; Porter, M. D. *Langmuir* **1988**, *4*, 365–385.
(41) Moulder, J. F.; Stickle, W. F.; Sobol, P. E.; Bomben, K. D. *Handbook of X-ray Photoelectron Spectroscopy*; Physical Electronics: Eden Prairie, MN, 1995.
(42) Kuhnle, A.; Linderoth, T. R.; Hammer, B.; Besenbacher, F. *Nature* **2002**, *415*, 891–893.
(43) Reichert, J.; Schiffrin, A.; Auwarter, W.; Weber-Bargioni, A.; Marschall, M.; Dell'Angela, M.; Cvetko, D.; Bavdek, G.; Cossaro, A.; Morgante, A.; Barth, J. V. *ACS Nano* **2010**, *4*, 1218–1226.
(44) Chen, Q.; Richardson, N. V. *Nat. Mater.* **2003**, *2*, 324–328.
(45) Holinga, G. J.; York, R. L.; Onorato, R. M.; Thompson, C. M.; Webb, N. E.; Yoon, A. P.; Somorjai, G. A. *J. Am. Chem. Soc.* **2011**, *133*, 6243–6253.
(46) Hung, A.; Mwenifumbo, S.; Mager, M.; Kuna, J. J.; Stellacci, F.; Yarovsky, I.; Stevens, M. M. *J. Am. Chem. Soc.* **2011**, *133*, 1438–1450.
(47) Petoral, R. M.; Uvdal, K. *Colloids Surf., B* **2002**, *25*, 335–346.
(48) Schiffrin, A.; Reichert, J.; Pennec, Y.; Auwrter, W.; Weber-Bargioni, A.; Marschall, M.; Dell'Angela, M.; Cvetko, D.; Bavdek, G.; Cossaro, A.; Morgante, A.; Barth, J. V. *J. Phys. Chem. C* **2009**, *113*, 12101–12108.
(49) Slojkowska, R.; Jurkiewicz-Herbich, M. *Colloids Surf., A* **2001**, *178*, 325–336.
(50) Uvdal, K.; Vikinge, T. P. *Langmuir* **2001**, *17*, 2008–2012.
(51) Wang, Y.; Niu, L.; Li, Y.; Mao, X.; Yang, Y.; Wang, C. *Langmuir* 2010, *26*, 16305–16311.
(52) Thermo Electron Corp., 2004.
(53) Bain, C. D.; Troughton, E. B.; Tao, Y. T.; Evall, J.; Whitesides, G. M.; Nuzzo, R. G. *J. Am. Chem. Soc.* **1989**, *111*, 321–335.
(54) Dubois, L. H.; Zegarski, B. R.; Nuzzo, R. G. *J. Am. Chem. Soc.* **1990**, *112*, 570–579.
(55) Moger, J.; Gribbon, P.; Sewing, A.; Winlove, C. P. *Biochim. Biophys. Acta* **2007**, *1770*, 912–918.
(56) Desamero, R. Z. B.; Kang, J.; Dol, C.; Chinwong, J.; Walters, K.; Sivarajah, T.; Profit, A. A. *Appl. Spectrosc.* **2009**, *63*, 767–774.
(57) Hernandez, B.; Pfluger, F.; Adenier, A.; Kruglik, S. G.; Ghomi, M. *J. Phys. Chem. B* **2010**, *114*, 15319–15330.
(58) Nucci, N. V.; Scott, J. N.; Vanderkooi, J. M. *J. Phys. Chem. B* **2008**, *112*, 4022–4035.
(59) Roepe, P.; Ahl, P. L.; Gupta, S. K. D.; Herzfeld, J.; Rothschild, K. J. *Biochemistry* **1987**, *26*, 6696–6707.
(60) Zinola, C. F.; Rodriguez, J. L.; Arevalo, M. C.; Pastor, E. *J. Electroanal. Chem.* **2005**, *585*, 230–239.
(61) Gupta, V. K.; Abbott, N. L. *Science* **1997**, *276*, 1533–1536.
(62) Skaife, J. J.; Abbott, N. L. *Chem. Mater.* **1999**, *11*, 612–623.
(63) Skaife, J. J.; Abbott, N. L. *Langmuir* **2001**, *17*, 5595–5604.
(64) Polossat, E.; Dozov, I. *Mol. Cryst. Liq. Cryst. Sci. Technol., A* **1996**, *282*, 223–233.
(65) Qi, H.; O'Neil, J.; Hegmann, T. *J. Mater. Chem.* **2008**, *18*, 374–380.
(66) Schreivogel, A.; Dawin, U.; Baro, A.; Giesselmann, F.; Laschat, S. *J. Phys. Org. Chem.* **2009**, *22*, 484–494.
(67) Thompson, M. P.; Lemieux, R. P. *J. Mater. Chem.* **2007**, *17*, 5068–5076.
(68) Zanchetta, G.; Giavazzi, F.; Nakata, M.; Buscaglia, M.; Cerbino, R.; Clark, N. A.; Bellini, T. *Proc. Natl. Acad. Sci. U.S.A.* **2010**, *107*, 17497–17502.
(69) Mecozzi, S.; West, A. P., Jr.; Dougherty, D. A. *Proc. Natl. Acad. Sci. U.S.A.* **1996**, *93*, 10566–10571.
(70) Mecozzi, S.; West, A. P., Jr.; Dougherty, D. A. *J. Am. Chem. Soc.* **1996**, *118*, 2307–8.
(71) Ohta, K.; Tominaga, K. *Chem. Phys.* **2007**, *341*, 310–319.
(72) Takahashi, R.; Noguchi, T. *J. Phys. Chem. B* **2007**, *111*, 13833–13844.
(73) Abramczyk, H.; Reimschussel, W. *Chem. Phys.* **1985**, *100*, 243–252.
(74) Jawed, I. *Bull. Chem. Soc. Jpn.* **1977**, *50*, 2602–2605.
(75) Arnett, E. M.; Mitchell, E. J.; Murty, T. S. S. R. *J. Am. Chem. Soc.* **1974**, *96*, 3875–3891.
(76) Lee, J.; Ross, R. T. *J. Phys. Chem. B* **1998**, *102*, 4612–4618.
(77) Gramstad, T.; Fuglevik, W. J. *Acta Chem. Scand.* **1962**, *16*, 1369–1377.
(78) Pace, C. N.; Horn, G.; Hebert, E. J.; Bechert, J.; Shaw, K.; Urbanikova, L.; Scholtz, J. M.; Sevcik, J. *J. Mol. Biol.* **2001**, *312*, 393–404.

(79) Ulman, A. *Chem. Rev.* **1996**, *96*, 1533–1554.
(80) Sellers, H.; Ulman, A.; Shnidman, Y.; Eilers, J. E. *J. Am. Chem. Soc.* **1993**, *115*, 9389–9401.
(81) Drawhorn, R. A.; Abbott, N. L. *J. Phys. Chem.* **1995**, *99*, 16511–16515.
(82) Fenter, P.; Eisenberger, P.; Liang, K. S. *Phys. Rev. Lett.* **1993**, *70*, 2447.
(83) Gupta, V. K.; Miller, W. J.; Pike, C. L.; Abbott, N. L. *Chem. Mater.* **1996**, *8*, 1366–&.
(84) Luk, Y. *J. Chem. Phys.* **2004**, *120*, 10792.
(85) Wade, L. G., Jr. *Organic Chemistry*; 5th ed.; Prentice Hall: Upper Saddle River, NJ, 2003.
(86) Razgulin, A. V.; Mecozzi, S. *J. Med. Chem.* **2006**, *49*, 7902–7906.
(87) Vogel, H. J. In *Methods in Enzymology*; Norman, J. O., James, T. L., Eds.; Academic Press: New York, 1989; Vol. 177, pp 263−282.
(88) Wojciechowski, M.; Grycuk, T.; Antosiewicz, J. M.; Lesyng, B. *Biophys. J.* **2003**, *84*, 750–756.